RSC Advances

ROYAL SOCIETY OF CHEMISTRY

www.rsc.org/advances

RSC Advance

RSCPublishing

ARTICLE

Precise Control of Nanoparticle Surface by Host-Guest Chemistry for Delivery to Tumor

Cite this: DOI: 10.1039/x0xx00000x

Hisato Matsui,[a] Motoki Ueda,[b] Isao Hara,[c] and Shunsaku Kimura*[,a]

Received 00th January 2012,
Accepted 00th January 2012

DOI: 10.1039/x0xx00000x

www.rsc.org/

Nanoparticles are prepared by host-guest chemistry using stereo-complex formation between the right-handed and the left-handed helical peptides. The host molecule is a 3rd generation polyamideamine dendrimer having 16 terminated right-handed helices. Three kinds of guest molecules are examined; poly(sarcosine)-*b*-(D-Leu-Aib)$_6$ (AB-LP), (poly(sarcosine))$_3$-*b*-(D-Leu-Aib)$_6$ (A_3B-LP), and (D-Leu-Aib)$_6$-*b*-(poly(sarcosine))$_3$ (A_3B-apLP). All the guest peptides associate stoichiometrically with the host dendrimer because of the stereo-complex formation. When A_3B-apLP associates with the host dendrimer, the conjugate shows a hydrodynamic diameter of 27 nm, which is explainable that the 16 guest peptides are incorporated in the host dendrimer with tight helix packing and the antiparallel helix dipole arrangement. The nanoparticles are labeled with indocyanine green fluorescence agent, and are applied for tumor imaging. Among them the conjugate with A_3B-apLP shows a long life time in the blood stream, and a good tumor/liver signal ratio. Further, the conjugate does not trigger the accelerated blood clearance phenomenon. Although these nanoparticles modified by the similar guest molecules should have similar surfaces, their in vivo disposition are found to be significantly affected.

Introduction

Nanoparticles have been attracting much attention in the field of the theranostics,[1] which is currently considered to be essential for the personalized medicine.[2–5] They can load various types of imaging agents and therapeutic agents. The nanoparticles loading imaging probes will provide information of the *in vivo* disposition, which can determine the appropriate dose for individuals and can predict adverse effects of the nanoparticles loading drugs. There is, however, a serious obstacle for nanoparticles to be used as a vehicle of the imaging and therapeutic agents, that is the pharmacokinetic changes of the nanoparticles between the first dose of the imaging nanoparticle and the following dose of the same nanoparticle or the therapeutic nanoparticle. The pharmacokinetic alterations can be caused by two reasons. One is the change of physical properties (particle size, structural stability, surface density, thickness of hydrophilic shell, half-life time in blood stream and so on) of the nanoparticle upon labelling and loading different agents for the diagnosis and the therapy on the nanoparticle. The other is the immune response to the nanoparticle, which is known as the accelerated blood clearance (ABC) phenomenon.[6–9] In order to solve out these difficulties, it is imperative to examine various types of the nanoparticles, and we prepared them here by using host-guest chemistry.

One typical example of nanoparticles is a polymeric micelle.[10] It is easy to load hydrophobic agents at the hydrophobic core of the core-shell type micelles and to insert functional polymer via a hydrophobic interaction. However, the size control is a difficult task because of swelling of the polymeric micelle with loading these agents[10] or changing the hydrophilic-hydrophobic balance by binding functional molecules. Further, modification of nanoparticle surface with a diagnosis probe affected the life time in the blood stream.[11] Aiming at solving these problems, we have proposed a novel molecular assembly using host-guest chemistry applied on a dendritic host scaffold, which makes it possible to construct one nanoparticle with keeping a defined number of the constituent amphiphilic polymers and the core size unchanged upon incorporation of functional groups. Accordingly, the dendritic core had eight amphiphilic polypeptides as a host molecule to incorporate eight amphiphilic polypeptides as a guest molecule.[12] These polypeptides have a helical hydrophobic block with opposite helicity, and these two types of helices forms stereo-complex at 1:1 stoichiometry.[12-15] We successfully prepared a polymeric nanoconjugate containing sixteen amphiphilic polypeptides under the host-guest chemistry. With a chemical modification of the guest amphiphilic polypeptide by a diagnostic or therapeutic agent, this type of nanoconjugate can therefore be functionalized with keeping the size unchanged due to the constant core size of dendritic host molecule and the defined number of guest peptides. Here, we extended this scheme to a dendrimer with sixteen amphiphilic polypeptides in combination with three types of the guest amphiphilic polypeptides to achieve a more precise molecular control of the nanoparticle (Fig. 1). In order to evaluate the nanoparticle properties precisely, we also examined on the availability of the nanoparticles for tumor imaging.

Results and Discussion

Self-assembling by host-guest chemistry

The association of the guest peptides (AB-LP, A_3B-LP and A_3B-apLP) with the host dendrimer (16RD) was analyzed by the dynamic light scattering (DLS) measurements with varying the feed molar ratios of the guest peptides against the host. In these combinations, there were three types of molecular assemblies coexisting in the mixtures, the assemblies of the pure guest, the pure host, and a mixtureof the guest and the host because these guests and the host are amphiphilic by themselves. The former two types of molecular assemblies became relatively a large size over 200 nm. The guest molecule alone formed a curved sheet of ca. 200 nm square as previously reported.[12,16-19] The host took a small disk-like structure which quickly grew into larger aggregates of ca. 200 nm size by itself, because the peripheral sixteen poly(sarcosine) chains of the host cannot shield the hydrophobic blocks inside.[12] On the other hand, upon association of the guest peptide with the host the molecular assemblies became smaller (Fig. 2).

A mixture of AB-LP and 16RD at the feed molar ratio of 16:1 formed a molecular assembly having a minimum diameter of 49 nm (Fig. 2a), suggesting that they should associate in a stoichiometric manner of 1:1 between the right-handed helices of 16RD and the left-handed helices of AB-LP as expected. With decreasing the ratios below 16:1, the hydrodynamic diameters became larger up to 200 nm which size corresponds to the molecular assembly of pure 16RD. The hydrodynamic diameters also became larger with increasing the ratios above 16:1 because the excess AB-LP generated curved sheets of 200 nm. It is considered therefore that 16RD cannot accommodate more than 16 mol equivalents of the guest peptides.

TEM images (Fig. 2b–d) supported the coexistence of these three kinds of molecular assemblies in the mixtures. Molecular assemblies of about 50 nm size were formed from a mixture of AB-LP and 16RD at a molar ratio of 16:1 (Fig. 2b). In addition to this size of molecular assemblies, large curved sheets coexisted when AB-LP and 16RD were mixed at a molar ratio of 32:1. The mixed solutions were filtered through cut-off membrane of 20 kDa to remove the molecular assemblies with sizes over 200 nm of 16RD or AB-LP, and the filtrates were subjected to CD measurements. The Cotton effects due to the remaining helicity of the guest (right-handed helix)-host (left-handed helix) conjugate decreased with increasing the ratios of the guest up to 16. Further increasing the ratios to 24 and 32 remained the Cotton effects nearly zero (Fig. S2 in Electronic Supplementary Information (ESI)), supporting that small conjugate was composed of 16RD and sixteen AB-LPs, and then that 16RD cannot accommodate the guest peptides more than 16 mol equivalents.

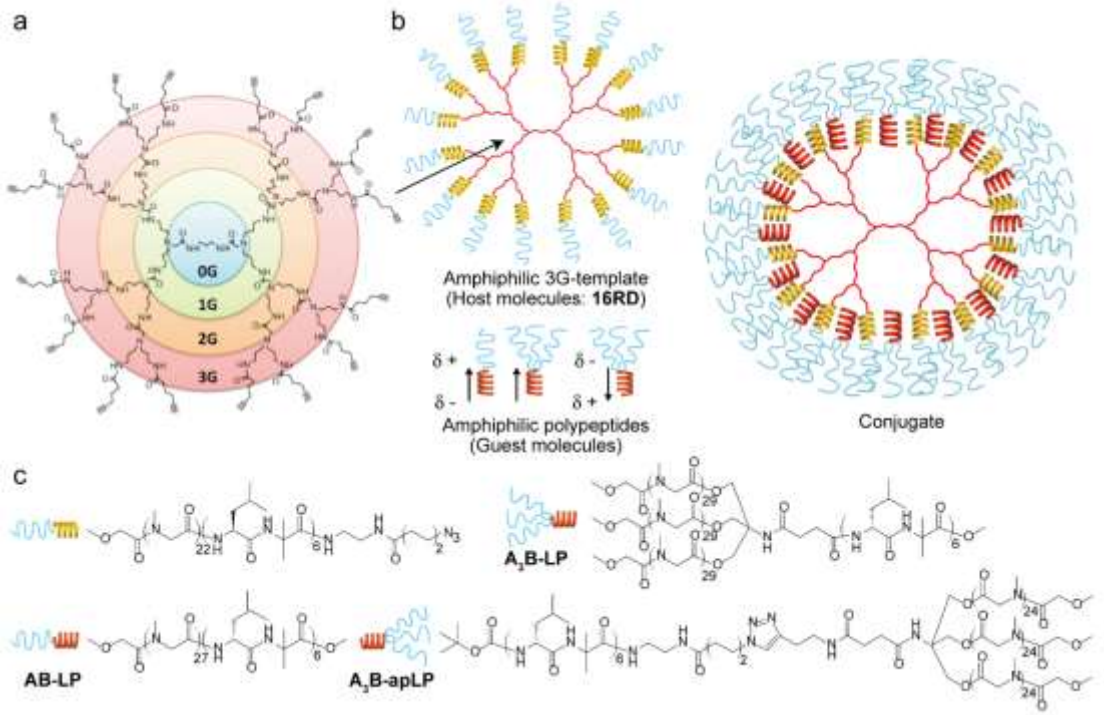

Fig. 1 Schematic illustration and chemical structure of host and guest molecules. Schematic illustration of 3rd generation dendrimer core (a), amphiphilic dendrimer template, three amphiphilic guest molecules and host-guest nanocunjugate (b). Chemical structure of amphiphilic three guest molecules (AB-LP, A_3B-LP, A_3B-apLP) (c)

The hydrodynamic diameter of 49 nm, however, is significantly

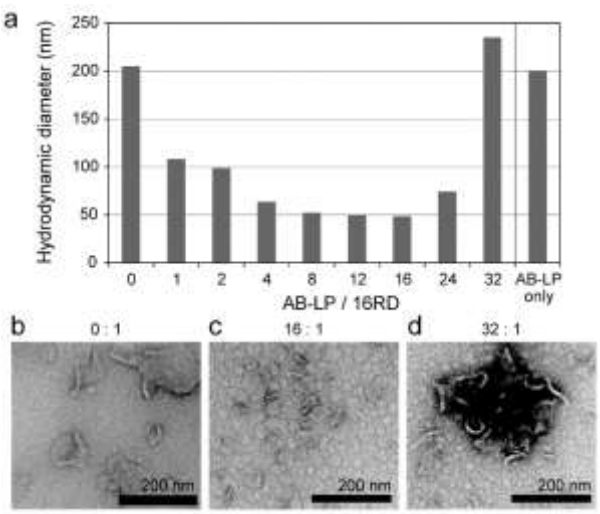

Fig. 2 Hydrodynamic diameters vs feed molar ratios of AB-LP/16RD by DLS measurement (a) and TEM images (negative staining with uranyl acetate) of molecular assembly prepared from a mixture of AB-LP and 16RD at molar ratio 0:1 (b), 16:1 (c) and 32:1 (d).

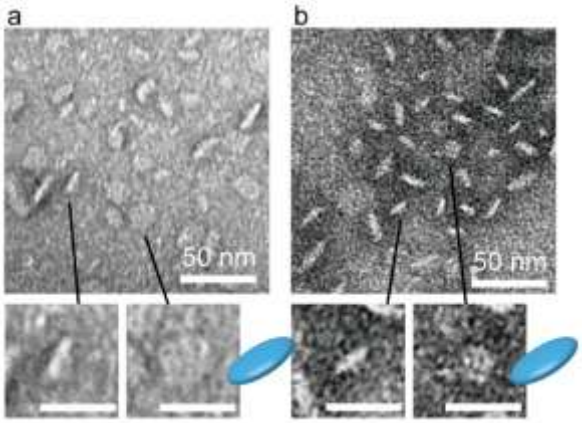

Fig. 3 TEM images of molecular assemblies prepared from a mixture of A_3B-LP/16RD (a) and A_3B-apLP/16RD (b) at molar ratio of 16:1, respectively. Magnified figures were shown at bottom. Scale bars in magnification were 25 nm.

larger than the estimated value of ca. 25–30 nm for the guest-host conjugate. TEM observations revealed that the guest-host conjugates aggregated to some extent in a time-dependent manner. It is therefore considered that the surface property of the AB-LP/16RD conjugate was not hydrophilic enough to shield the hydrophobic helix layer of the conjugate. Indeed, the morphology of the conjugate was found to be disk-like, which has been frequently observed with lower generation dendrimers due to the low density of the dendritic chains inside. In order to suppress the aggregation of the conjugate, we therefore designed the A_3B-type guests.

The hydrodynamic diameters of the A_3B-type guest peptides/the host (16RD) conjugate were measured with varying the ratios of the guest against the host. The minimum hydrodynamic diameters were obtained with the additions of 16 mol equivalent A_3B-LP and 14 mol equivalent A_3B-apLP to be 32 nm and 27 nm, respectively (Fig. S3 in ESI). Thus, these guest peptides also associated stoichiometrically with the host dendrimer on the basis of the stereo-complex formation between the right-handed and the left-handed helices. Furthermore, at mixing ratios of 8:1, 12:1 and 14:1, the guest-host associates also kept the similar size (Fig. S3), suggesting that the dendrimer core should be a primary determinant of the associate sizes. TEM observation revealed that the conjugates still kept the disk-shaped morphology based on the wormlike-shaped side-view and the sphere-shaped top-view (Fig. 3), but no aggregation was detected at room temperature for 24 h. The local high density of poly(sarcosine) chains of the A_3B-type peptides should provide sufficient hydrophilicity. Not sphere-shaped but disk-shaped assembly may be obtained because the 3G dendrimer was not sphere-shape but ellipsoid-shape.[17]

The hydrodynamic diameter of 27 nm for the A_3B-apLP/16RD conjugate corresponds just to the estimated diameter where the guest helices and the host helices take interdigitated side-by-side arrangement with antiparallel dipole orientation (Fig. 4). On the other hand, the A_3B-LP/16RD conjugate showed a slightly larger diameter of 32 nm, which may be explained by the dipole-dipole interaction working to thicken the helical peptide layer in the conjugate as follows. When A_3B-LP is inserted into the surface peptide region of 16RD, A_3B-LP should take an orientation of keeping the bulky A_3-block outside of 16RD. The helix block of A_3B-LP then prefers head-to-tail arrangement with the helix block of 16RD in order to avoid a side-by-side arrangement where the parallel arrangement of helix dipoles

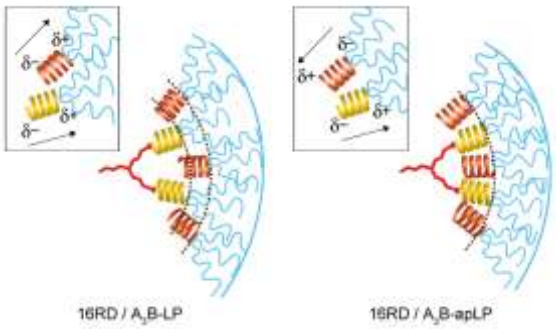

Fig. 4 Illustrations of molecular packing in hydrophobic layer in case of A_3B-LP/16RD (a) and A_3B-apLP/16RD (b). Arrows mean the dipole moments along hydrophobic α-helices.

should destabilize the helix packing in the conjugate. It is therefore considered that the steric effect in the association of the guest peptide with the host dendrimer should take priority, and the following dipole-dipole interaction should decide the helix packing of the side-by-side or the head-to-tail arrangement in the conjugates (Fig. 4).[20] Accordingly, as far as the 2nd generation[12] and the 3rd generation dendrimers are concerned, there is no difference about the host-guest chemistry in the present molecular systems.

***In vivo* disposition**

The A_3B-LP/16RD conjugate and the A_3B-apLP/16RD conjugate have the same constituents except the direction of helix dipoles of the guest being parallel or antiparallel to that of the host. The structural difference makes the size of the A_3B-LP/16RD conjugate slightly larger than the A_3B-apLP/16RD conjugate. These two types of the conjugates were labeled with ICG and examined on tumor imaging of mice. Even though the surface modification between these two conjugates looks very similar, they showed a different behavior about *in vivo* pharmacokinetics.

A mixture of 16RD, A_3B-apLP and ICG-LP (Fig. 5a) at a ratio of 1:14:0.16 generated the ICG-labeled conjugate with a diameter of 27 nm, which was the same size of the A_3B-apLP/16RD conjugate at a mixing ratio of 1:14 (Fig. 5b). This observation is a good evidence for the present guest-host chemistry in the preparation of functionalized nanoparticles being very useful for the size control. The buffered solutions of the ICG-labeled conjugates were injected to tumor bearing mice from the tail vein and NIRF images were taken by Shimadzu Clairvivo OPT (Fig. 5). When the images at 9 h after the injection were compared, the whole body fluorescence intensity was significantly larger with the A_3B-apLP/16RD conjugate than the A_3B-LP/16RD conjugate reflecting that the circulating amount of the A_3B-apLP/16RD conjugate in the blood stream was larger than that of the A_3B-LP/16RD conjugate (Fig. 5c and 5d). This is because the A_3B-LP/16RD conjugate is initially more easily captured by liver to reduce the concentration in the

blood stream as shown in Fig. 5e. As a result, the accumulation amount of the A_3B-apLP/16RD conjugate in the tumor was nearly two-times higher than that of the A_3B-LP/16RD conjugate. The tumor/liver signal ratio is also better with the A_3B-apLP/16RD conjugate than the A_3B-LP/16RD conjugate (Fig. 5e). The stability of the A_3B-apLP/16RD conjugate in the blood stream may be attributable to 1.3-times higher surface density of poly(sarcosine) chains with the A_3B-apLP/16RD conjugate than the A_3B-LP/16RD conjugate on the basis of a simple calculation of the surface areas of the diameters of 27 nm and 32 nm, respectively.

Further, the antiparallel packing of helix dipoles in the A_3B-apLP/16RD conjugate may contribute to the physical stability in the blood stream. The physical stability which means that the ICG-LP stayed in the conjugate in the blood stream is indeed supported by the observation that the accumulation amount in the tumor site increased with time up to 20 h.

The A_3B-apLP/16RD conjugate was examined about the in vivo pharmacokinetics upon repeated administrations. It has been reported that the PEGylated liposome and the polymeric micelles at the second dose were immediately captured by liver even though they showed a long life time in the blood stream at the first dose.[6–9] This type of alteration in the pharmacokinetics is called as the accelerated blood clearance (ABC) phenomenon. When the A_3B-apLP/16RD conjugate was dosed at 7 days after the first injection, the time-profiles of the accumulation in tumor, liver, and background coincided just with those at the first dose (Fig. 6). The reason for no ABC phenomenon with the A_3B-apLP/16RD conjugate remains to be solved out, but this type of the conjugate should be useful as a nanocarrier platform for clinical tumor diagnostics and therapy, which can be attained by loading the diagnostic or therapeutic agent on the guest peptide. With this platform, the nanoparticles can keep the size on the functionalization without immune response on multiple administrations.

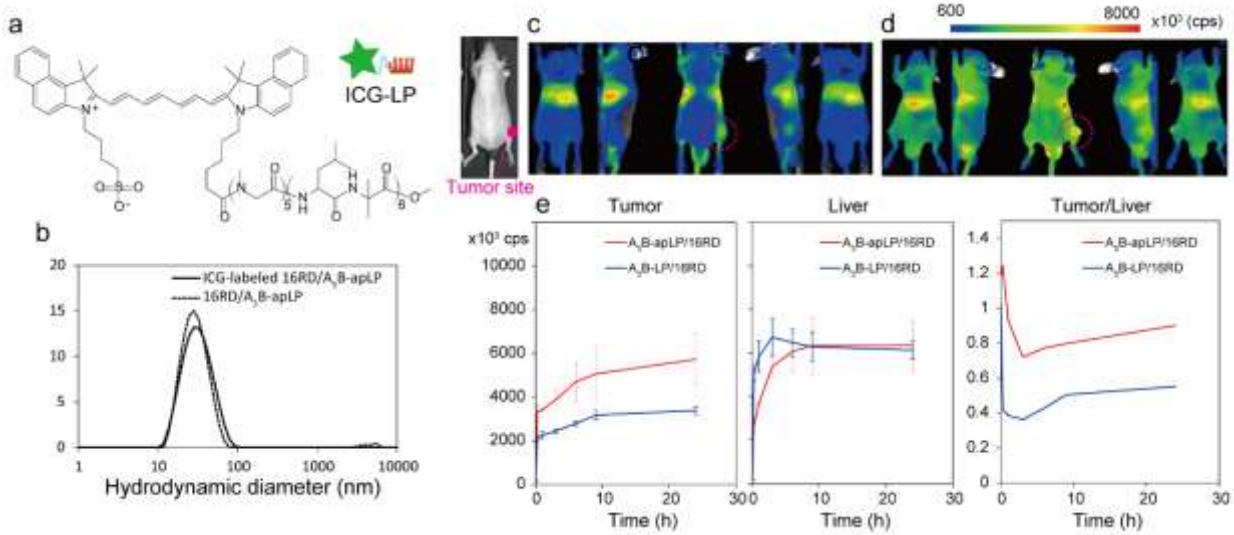

Fig. 5 Chemical structure of ICG-labeled amphiphiles, ICG-LP (a), DLS profiles of molecular assemblies prepared from a mixture of A_3B-apLP and 16RD at mixing ratio of 14:1 with and without ICG-LP at 0.16 eq. (b). *In vivo* NIRF imaging results (c–e). NIRF images of nanocarriers from A_3B-LP/16RD/ICG-LP (c) and A_3B-apLP/16RD/ICG-LP (d) after 9 h from administration. The region of interest (ROI) at tumor site, liver site and tumor/liver NIRF intensity ratio (e).

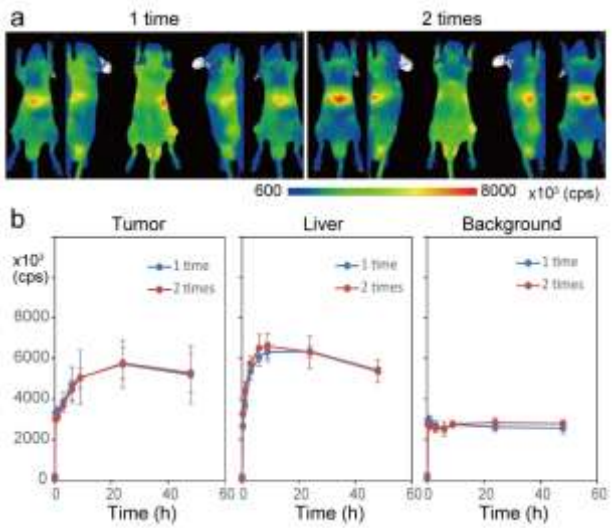

Fig. 6 NIRF images of nanocarrier from A_3B-apLP/16RD/ICG-LP after 9 h from 1st and 2nd administrations (a) and the time profiles of ROI at tumor site, liver site and background (left-leg site) (b).

Conclusions

We demonstrated a useful nanocarrier whose diameter is less than 30 nm. Various chemical agents can be loaded on the nanocarrier with a defined concentration and keeping the size unchanged. The nanocarrier showed a long life time in the blood stream, and no ABC phenomenon was triggered. Tumor imaging is available with the nanocarrier due to the enhanced permeability and retention effect. The chemistry of the nanocarrier is based on the stereocomplex formation between the right-handed and the left-handed helices. The 16 guest peptides can be accommodated in the 16-helix terminated dendrimer due to the stereo-complex formation. The surface of the conjugate is covered with poly(sarcosine) chains densely due to the A_3B-type molecular architecture. The conjugate was highly stable in the blood stream because of the tight helix

packing and antiparallel arrangement of the helix dipoles in the conjugate. We tried here functionalization of the conjugate with using an ICG-modified guest peptide for tumor imaging. We think various functionalization will be available with just changing the ICG moiety with other agents with keeping the size, a long life time in the blood stream, and no ABC phenomenon of the conjugate.

Experimental Section

Materials and Methods

Dendrimer (Host molecule) and Amphiphilic Helical Peptides (Guest molecules)

The 3rd generation (3G) PAMAM dendrimer template (16RD) and three kinds of amphiphilic polypeptides of Sar_{27}-*b*-(D-Leu-Aib)$_6$ (AB-LP), $(Sar_{29})_3$-*b*-(D-Leu-Aib)$_6$ (A_3B-LP), and (D-Leu-Aib)$_6$-*b*-$(Sar_{24})_3$ (A_3B-apLP) (Fig. 1) were synthesized in accordance with the supporting information and previous papers.[10,16–18] 16RD (16 right-handed-helices-modified dendrimer) was synthesized by using the click reaction between the 16 terminal azido groups of the dendrimer and the acetylene group at the *C*-terminal of the right-handed amphiphilic polypeptide. AB-LP (AB-type left-handed helical peptide) have one hydrophilic poly(sarcosine) chain (A) and one left-handed helical hydrophobic peptide (B). On the other hand, A_3B-LP (A_3B-type left-handed helical peptide) and A_3B-apLP (A_3B-type anti-parallel left-handed helical peptide) are composed of three poly(sarcosine) chains (A_3) and one left-handed helix (B). The structural difference between A_3B-LP and A_3B-apLP is that three poly(sarcosine) chains are attached at either *N*-terminal or the *C*-terminal of the hydrophobic helix peptide. Poly(sarcosine) was used due to the thicker polymer chain than poly(ethylene glycol), which contributes to formation of a dense hydrophilic layer around the molecular assemblies. The syntheses of all compounds were confirmed by ^{1}H NMR and MALDI-TOF MASS analyses.

Synthesis of ICG-Sar_5-(D-Leu-Aib)$_6$-OMe (ICG-LP)

ICG-LP (Fig. 5a) was synthesized according to Scheme S3 in ESI. To a solution of Sar-NCA (6.19 mg, 53.8 μmol) in distilled DMF (150 μL), a solution of the desalted compound of H-(D-Leu-Aib)$_6$-OMe (6.57 mg, 5.38 μmol) in distilled DMF (50 μL) was added under Ar atmosphere, and the mixed solution was stirred at the room temperature for 15 h. After the complete consumption of Sar-NCA, ICG-sulfo-OSu (1.00 mg, 1.08 μmol) and DCC (0.44 mg, 2.15 μmol) were added to the solution in this order and stirred at the room temperature for 25 h under Ar atmosphere. The solvent was evaporated, and the residue was dissolved in DMF and purified by Sephadex LH20 column. The chain length of poly(sarcosine) was determined by integration intensity ratio between Sar NCH_2 and Leu $CH_2(CH_3)_2$ in the ^{1}H NMR spectrum. The yield was determined by the absorbed light intensity of ICG moiety in DMSO (absorption wavelength: 794 nm). Yield: 2.33 mg, 1.02 nmol (95 %) (2 steps).

Preparation of Molecular Assemblies

The molecular assemblies were prepared by the injection method.[10] 16RD (10 mg) and the amphiphilic block polypeptides (5 mg) were dissolved in ethanol (100 μL), respectively to prepare their stock solutions. The each mixed solution of the amphiphilic block-polypeptide solution (2.5 μL) and the 16RD solution with the molar ratio of 0:1, 1:1, 2:1, 4:1, 8:1, 16:1, 24:1, 32:1 was injected into a buffer (0.5 mL, 10 mM Tris-HCl, pH 7.4) with stirring at 4 °C.

Preparation of ICG-labeled molecular assemblies

An ethanol solution (10 μL) of 16RD (6.1 nmol), A_3B-LP or A_3B-apLP (85.4 nmol), and ICG-LP (1 nmol) at a molar ratio of 1:14:0.16 was injected into a saline (0.5 mL) in a sample vial at 4 °C. This dispersion was kept stirring at 4 °C for 30 min, allowed to reach room temperature, filtered through a membrane filter (polyethersulfone, 100 nm), and then used for fluorescent analysis and in vivo imaging experiment.

Transmission Electron Microscopy (TEM)

TEM images were taken using a JEOL JEM-2000EXII at an accelerating voltage of 100 kV. A drop (2 μL) of dispersion was mounted on a carbon-coated Cu grid and stained negatively with 2 % uranyl acetate, followed by suction of the excess fluid with a filter paper.

Circular Dichroism (CD)

CD measurements were carried out on a JASCO J600 spectropolarimeter with an optical cell of 0.1 cm optical path length at room temperature.

Dynamic Light Scattering (DLS)

The hydrodynamic diameter of assemblies were measured by DLS-8000KS (Photal Otsuka Electronics) using He-Ne laser. Before DLS measurement, each prepared sample was filtered by 0.20 μm PVDF (polyvinylidene fluoride) syringe filter (GE Healthcare UK limited).

Cell culture

Pancreatic carcinoma (SUIT-2/pEF/LUC) cell line was maintained at 37 °C with 5% FBS (Nacalai Tesque, Inc. Kyoto, Japan) in Dulbecco's modified Eagle's medium (DMEM, Gibco, Invitrogen Corp. USA) supplemented with GlutaMAX™-I supplement (2 mmol/L, Gibco, Invitrogen Corp., USA), Plasmocin™ prophylactic (5 μg/mL, Nacalai Tesque, Inc., Kyoto, Japan), penicillin (100 U/mL), and streptomycin (100 mg/mL).

In vivo near-infrared fluorescence (NIRF)-imaging with ICG-labelled assemblies

SUIT-2/pEF/LUC cells (5×10^5 cells) were dissolved in phosphate-buffered saline (PBS, 20 μL), and subcutaneously inoculated into right femoral region of 7-week-old BALB/c nu/nu mice (n=4 per group). The molecular assembly composed of 16RD and A_3B-LP or A_3B-apLP (5 mg/kg, 100 μL) was injected via tail vein to the mice at 1 week after the tumor transplantation. The second dose of the ICG-labelled molecular assembly (5 mg/kg, 100μL) was injected to the mice at 1 week after the first dose. The injected ICG amount was set to be 5 nmol/kg. NIRF images were taken at 15 min, 1 h, 3 h, 6 h, 9 h, and 24 h after the second dose. During the imaging process, the mice were held on the imaging stage under anesthetized condition with 2.5% of isoflurane gas in air flow (1.5 L/min). The pseudo images were constructed from the photon counts.

Ethics

All of our in vivo animal experiments were approved by the Animal Research Committee of Kyoto University. Animals were treated humanely.

Acknowledgements

This study is a part of translational research network program by MEXT, a part of S-innovation by JST, and a part of the innovative techno-hub for integrated medical bio-imaging of the project for developing innovation systems by MEXT.

Notes and references

[a] Department of Material Chemistry, Graduate School of Engineering, Kyoto University, Kyoto-Daigaku-Katsura, Nishikyo-ku, Kyoto, 615-8510, Japan.
[b] Clinical Division of Diagnostic Radiology, Kyoto University Hospital, 54 Shogoin Kawara-cho, Sakyo-ku, Kyoto, 606-8507, Japan.
[c] Technology Research Laboratory, Shimadzu Corporation, Kyoto 619-0237, Japan

† Electronic Supplementary Information (ESI) available: [details of any supplementary information available should be included here]. See DOI: 10.1039/b000000x/

1. J. Xie, S. Lee and XY. Chen, *Adv. Drug Deliv. Rev.*, 2010, **62**, 1064.
2. Z. Wang, G. Niu and XY. Chen, *Pharm. Res-Dordr*., 2014, **31**, 1358.
3. T. Moore, HY. Chen, R. Morrison, FL. Wang, JN. Anker and F. Alexis, *Mol. Pharmaceut.*, 2014, **11**, 24.
4. KY. Choi, G. Liu, S. Lee and XY. Chen, *Nanoscale*. 2012, **4**, 330.
5. N. Ahmed, H. Fessi and A. Elaissari, *Drug Discov. Today*, 2012, **17**, 928.
6. M. Yokoyama, *J. Drug Target*, 2014, **22**, 576.
7. E. Hara, M. Ueda, CJ. Kim, A. Makino, I. Hara, E. Ozeki and S. Kimura, *J. Pept. Sci*., 2014, **20**, 570.
8. H. Koide, T. Asai, K. Hatanaka, T. Urakami, T. Ishii, E. Kenjo, M. Nishihara, M. Yokoyama, T. Ishida, H. Kiwada and N. Oku, *Int. J. Pharm*., 2008, **362**, 197.
9. T. Ishida, M. Harada, XY. Wang, M. Ichihara, K. Irimura and H. Kiwada, *J. Control. Release*, 2005, **105**, 305.
10. B. F. Lin, R. S. Marullo, J. F. Robb, D. V. Krogstad, P. Antoni, D. J. Hawker, L. M. Campos, and M. V. Tirrell, *Nano Lett*., 2011, **11**, 3946.
11. A. Uesaka, I. Hara, T. Imai, J. Sugiyama, and S. Kimura, *RSC Adv*., **5**, 14697.
12. H. Matsui, M. Ueda, A. Makino and S. Kimura, *Chem. Commun*., 2012, **48**, 6181.
13. M. Ueda, A. Makino, T. Imai, J. Sugiyama and S. Kimura, *Soft Matter*, 2011, **7**, 4143.
14. M. Ueda, A. Makino, T. Imai, J. Sugiyama and S. Kimura, *Langmuir*, 2011, **27**, 4300.
15. M. Ueda, A. Makino, T. Imai, J. Sugiyama and S. Kimura, *Polym. J*., 2013, **45**, 509.
16. A. Uesaka, M. Ueda, A. Makino, T. Imai, J. Sugiyama and S. Kimura, *Langmuir*, 2014, **30**, 1022.
17. T. Kanzaki, Y. Horikawa, A. Makino, J. Sugiyama and S. Kimura, *Macromol. Biosci*., 2008, **8**, 1026.
18. M. Ueda, A. Makino, T. Imai, J. Sugiyama and S. Kimura, *J. Pept. Sci*., 2011, **17**, 94.
19. M. Ueda, A. Makino, T. Imai, J. Sugiyama and S. Kimura, *Chem. Commun*. 2011, **47**, 3204.
20. S. Kimura, *Org. Biomol. Chem*., 2008, **6**, 1143.

